

Article

Effect of Conformational Entropy on the Nanomechanics of Microcantilever-Based Single-Stranded DNA Sensors

Zou-Qing Tan ^{1,3} and Neng-Hui Zhang ^{1,2,*}

¹ Shanghai Key Laboratory of Mechanics in Energy Engineering, Shanghai Institute of Applied Mathematics and Mechanics, Shanghai University, Shanghai 200072, China;

E-Mail: zqtan@cczu.edu.cn

² Department of Mechanics, College of Sciences, Shanghai University, Shanghai 200444, China

³ College of Mechanical Engineering, Changzhou University, Changzhou 213016, China

* Author to whom correspondence should be addressed; E-Mail: nhzhang@shu.edu.cn;

Tel.: +86-21-66132303; Fax: +86-21-66132303.

Received: 26 May 2014; in revised form: 21 July 2014 / Accepted: 25 August 2014 /

Published: 15 September 2014

Abstract: An entropy-controlled bending mechanism is presented to study the nanomechanics of microcantilever-based single-stranded DNA (ssDNA) sensors. First; the conformational free energy of the ssDNA layer is given with an improved scaling theory of thermal blobs considering the curvature effect; and the mechanical energy of the non-biological layer is described by Zhang's two-variable method for laminated beams. Then; an analytical model for static deflections of ssDNA microcantilevers is formulated by the principle of minimum energy. The comparisons of deflections predicted by the proposed model; Utz–Begley's model and Hagan's model are also examined. Numerical results show that the conformational entropy effect on microcantilever deflections cannot be ignored; especially at the conditions of high packing density or long chain systems; and the variation of deflection predicted by the proposed analytical model not only accords with that observed in the related experiments qualitatively; but also appears quantitatively closer to the experimental values than that by the preexisting models. In order to improve the sensitivity of static-mode biosensors; it should be as small as possible to reduce the substrate stiffness.

Keywords: biosensor; conformational entropy; principle of minimum energy; two-variable method

1. Introduction

In recent years, microcantilever-based biosensors as a versatile platform for label-free biodetection have attracted much attention [1–3]. Such devices can either be static-mode (bending) sensors or dynamic-mode (resonance frequency variation) sensors. The low-cost sensors exhibit fast response, high sensitivity and suitability for parallelization into arrays and allow for a wide range of analyses, such as gene mutation [1], DNA hybridization [4] and protein-ligand interactions [5].

Experiments showed that DNA adsorption on a microcantilever beam can cause the cantilever to deflect. As the biomolecules bind, the cantilever deflection is developed due to surface stress variation. However, the physical mechanisms underlying the mechanical responses of microcantilevers to the biomolecular reactions remain an extensively argued issue. Based on different experiments at different conditions, the mechanisms were supposed to be either electrostatic and steric forces [4], or conformational entropy and intermolecular energetic [6], or physical steric crowding [7], or hydration forces [8]. These bending-causing factors are likely to be important to different degrees in different situations.

The challenge of theoretical modeling is that microcantilever-based DNA sensors are essentially multiscale systems in which molecular-level signals are transduced to mesoscopic elements, to allow readout by macroscopic measurement techniques (e.g., STM, ATM, optical tweezers) [9]. Different from traditional (plane or cylindrical or spherical) hard substrates, a microcantilever-based DNA sensor is a kind of biochemical-mechanical coupling system: when DNA chains are grafted onto a surface of a cantilever, if the bending stiffness of the substrate is sufficiently low, entropic driving forces within the DNA biofilm cause the cantilever to deflect. Conversely, the effect of cantilever deformation also influences the conformation of the biofilm (e.g., thickness of DNA biofilm). In addition, a microcantilever-based DNA sensor typically is a multilayered structure, including a DNA-, Si- or SiN_x-, Au-, Cr- or Ti-layer in a buffer solution environment. Recently, some theoretical methods have been presented to understand this mechanical behavior, such as liquid crystal theory [10,11], flexoelectric membrane theory [12], surface energy [13] and classical density functional theory [14].

In contrast with double-stranded DNA (dsDNA), there is relatively little information about the segment-segment interactions in single-stranded DNA (ssDNA) [10]. Zhang *et al.* [15] developed a phenomenological model to interpret this phenomenon considering the piezoelectric effect. Curve fitting with the related experimental data showed that the sign of the piezoelectric constant of ssDNA biofilm may control the deflection direction of ssDNA sensors. However, it is difficult to judge if the values of the fitting parameters are acceptable from a physical point of view. According to Daoud–Cotton’s model for cylindrical polymer brushes, Hagan *et al.* [10] presented a simplified two-layered model to investigate the effect of conformational entropy on the deflection of a microcantilever-based ssDNA sensor by the principle of minimum energy. Utz and Begley [16] formulated a relationship between molecular properties and surface stress induced by adsorption considering the thermal blob. The variation of surface stress during the adsorption-induced bending process is simplified as an external axial force/moment exerted on the cantilever [17]. However, they do not consider the effect of cantilever deformation on the conformational entropy of the biofilm. In addition, the above-mentioned theories neglected the dedication of coating thin layers to the

mechanical energy of biosensors. In this paper, we will formulate an alternative mathematical model for microcantilever-based ssDNA sensors.

This paper is limited to theoretically studying the influence of conformational entropy on the nanomechanical behaviors of a microcantilever-based ssDNA sensor by the principle of minimum energy. First, the conformational free energy of the ssDNA layer is obtained by an extended scaling theory, considering the curvature effect. Second, Zhang's two-variable method is used to describe the deformation field and the mechanical energy of non-biayers. Third, an analytical model for deflections of a ssDNA microcantilever is formulated by the principle of minimum energy, and the effects of DNA biofilm properties (including packing density, chain length and Flory parameter) and substrate properties (including thickness and elastic modulus) on deflections are discussed. In addition, the deflections predicted by the present model, Utz–Begley's model and Hagan's model are compared.

2. Theoretical Model

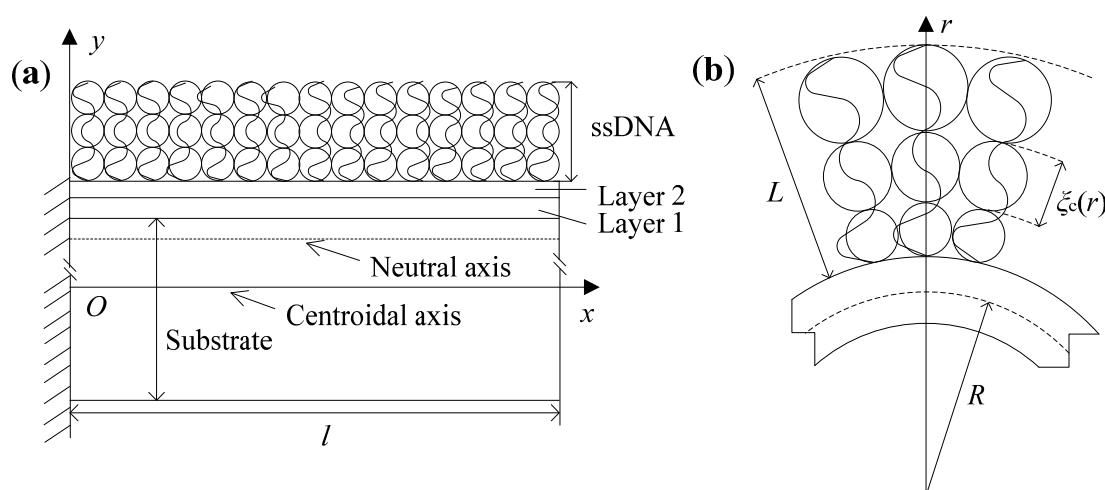
As shown in Figure 1a, a microcantilever-based DNA sensor is a typically laminated structure, which consists of two parts: DNA biofilm and non-biayers. The DNA layer can be viewed as a semidilute polymer solution. The non-biayers include Au-, Ti- or Cr- and Si or SiN_x-layers. The centroidal axis of the cantilever is taken as the coordinate axis x ; its vertical direction along the cantilever thickness is consistent with that of the coordinate axis y . Here, l , b and h are the length, width and thickness, respectively; h_s , h_1 and h_2 represent the respective thicknesses, and $h = h_s + h_1 + h_2$; E_s , E_1 and E_2 are the respective elastic moduli.

Since the microcantilever-based DNA sensor consists of two parts, DNA biofilm and non-biayers, the total free energy of the cantilever can be written as:

$$\Pi = U_{\text{DNA}} + U_{\text{bend}} \quad (1)$$

where U_{DNA} is the conformational free energy of DNA biofilm and U_{bend} is the mechanical energy of non-biayers.

Figure 1. Schematic showing a microcantilever-based DNA sensor and its coordinate system: (a) before deformation; (b) after deformation.



2.1. Conformational Free Energy

Self-assembled monolayers (SAMs) of ssDNA probes immobilized on one surface of microcantilevers form a dense polymer brush layer [8]. Because ssDNA has a much shorter persistence length (0.75 nm) than dsDNA (50 nm), conformational entropy effects are assumed to be much larger for ssDNA. Therefore, although an ssDNA molecule in an aqueous environment is a charged polymer (at moderate pH values), it still follows a random walk behavior in a semi-dilute monolayer regime if we assume that the interactions are sufficiently weak. Perhaps the treatment of charged polymers by the scaling theory is problematic, due to the long-range nature of the electrostatic interaction. However, at sufficient salt concentrations, with Debye lengths of the order of a few nanometers, the scaling theory can still provide an acceptable approximation. According to the scaling theory of polymer brushes, DNA biofilm can be regarded as a semidilute polymer solution [16]. In this approach, a salt solution of ssDNA is envisioned as a succession of units or “blobs” of a correlation length ξ_c . DNA chains form a surface film with close-packed correlation blobs emanating from the substrate, as shown in Figure 1b. Here, the surface area at any radius r is equal to the cross-sectional area of a blob of the correlation length times the number of chains [18].

$$\frac{rS}{\rho} = \xi_c^2 N_p \quad (2)$$

where S is the surface area of cantilevers before deformation, and $S = lb$; ρ is the curvature radius at the neutral axis (for zero normal strain); N_p is the number of chains, and $N_p = S\eta$, in which η is the packing density of DNA chains.

From Equation (2), the correlation length at any radius r is obtained as follows:

$$\xi_c(r) = \sqrt{\frac{r}{\rho\eta}} \quad (3)$$

On a shorter length scale, each of the correlation blobs contains a chain of thermal blobs, which are close-packed in a poor solvent and expanded to a self-avoiding random walk in a good solvent. The thermal blob size is related to the Flory interaction parameter χ [16].

$$\xi_T = \frac{a}{|1 - 2\chi|} \quad (4)$$

where a is the size of a single segment of the DNA chain.

In a ssDNA brush, the chains form a surface biofilm of correlation blobs. Scaling theory predicts a concentration profile in the form of a step function. The thickness of DNA biofilm h_{DNA} can be expressed as [16]:

$$h_{\text{DNA}} = \frac{N\xi_c(r_{\text{top}})}{g_T g_c} \quad (5)$$

where N is the number of nucleotides per DNA chain; g_T is the number of thermal blobs per correlation blob, and $g_T = (\xi_T / a)^2$; g_c is the number of segments per thermal blob, and $g_c = (\xi_c / \xi_T)^{1/\nu}$, in which ν is the scaling exponent depending on the long-range interactions along

the chain axis; r_{top} is the radial distance at the top surface of DNA biofilm, and $r_{top} = R + h/2 + h_{DNA}$, in which R is the curvature radius at the centroidal axis.

From Equation (5), the thickness of DNA biofilm h_{DNA} can be rewritten as:

$$h_{DNA} = h_{DNA}^* \left(\sqrt{\frac{R + h/2 + h_{DNA}}{\rho}} \right)^{(v-1)/v} \tag{6}$$

where $h_{DNA}^* = aN \left(a\sqrt{\eta} \right)^{(1-v)/v} |1 - 2\chi|^{2-1/v}$ represents Utz–Begley’s prediction for the thickness of DNA biofilm when the curvature effect of the substrate is neglected [16].

In the limit of relatively short chains, the thickness of the DNA biofilm is much smaller than the curvature radius of the cantilever, $h_{DNA} / \rho \ll 1$. By expanding the right term of Equation (6) as to h_{DNA} / ρ and abandoning the terms of second and higher order, one can obtain:

$$h_{DNA} = \frac{h_{DNA}^* \left[(R + h/2) / \rho \right]^{\frac{v-1}{2v}}}{1 + \frac{1-v}{2v} \frac{h_{DNA}^*}{\rho} \left[(R + h/2) / \rho \right]^{\frac{v+1}{2v}}} \tag{7}$$

In a good solvent, the conformational free energy of DNA biofilm U_{DNA} relative to $k_B T$ is equal to the number of correlation blobs n_{Blob} [19]. By integration across the biofilm thickness, the conformational free energy of DNA biofilm is given as:

$$U_{DNA} = k_B T n_{Blob} = k_B T \int_{R+h/2}^{R+h/2+h_{DNA}} \frac{3rS}{4\pi(\xi_c/2)^3 \rho} dr \tag{8}$$

where k_B is the Boltzmann constant and T is the absolute temperature.

Substituting Equation (3) into (8) yields:

$$U_{DNA} = \frac{6\sqrt{2}}{\pi} k_B T S \eta^{3/2} \rho^{1/2} \left(\sqrt{2R + h + 2h_{DNA}} - \sqrt{2R + h} \right) \tag{9}$$

In the case of small deflection, $h_{DNA} / (R + h/2)$ is a small quantity, by the method of Taylor series expansion, from Equation (9), the first-order approximation for the conformational free energy of DNA biofilm is obtained as:

$$U_{DNA} = \frac{6\sqrt{2} k_B T S \eta^{3/2} \rho^{1/2} h_{DNA}}{\pi \sqrt{2R + h}} \tag{10}$$

In order to describe the deformation of laminated beams, Zhang’s two-variable method [20–25] will be used. The normal strain at the location y is given as:

$$\varepsilon = \varepsilon_0 + y\kappa \tag{11}$$

where κ is the curvature at the neutral axis, and $\kappa = -1/\rho$; ε_0 is the normal strain at the coordinate axis x . Let $\varepsilon = 0$; the location of neutral axis can be obtained:

$$y_c = \epsilon_0 \rho \tag{12}$$

Therefore, the curvature radius at the centroidal axis is given as:

$$R = \rho(1 + \epsilon_0) \tag{13}$$

Substituting Equations (7) and (13) into (10) yields:

$$U_{DNA} = \frac{12 k_B T S \eta^{3/2} \nu \rho h_{DNA}^* [1 + \epsilon_0 + h / (2\rho)]^{-\frac{1}{2\nu}}}{\pi 2\nu \rho + (1 - \nu) h_{DNA}^* [1 + \epsilon_0 + h / (2\rho)]^{-\frac{\nu+1}{2\nu}}} \tag{14}$$

From the above-mentioned expression, we can see that the conformational free energy of DNA biofilm on deformable substrates depends not only on the chemical/physical properties of DNA biofilm, but also on mechanical properties of cantilevers. In fact, the cantilever beam is a kind of deformable structure. When the cantilever bends, the conformational free energy of DNA biofilm on a soft substrate will also change correspondingly. This is quite different from that on a stiff substrate, where, according to Equations (7) and (14), when $\rho \rightarrow +\infty$ and $\epsilon_0 \rightarrow 0$, $U_{DNA} \rightarrow 6k_B T S \eta^{3/2} h_{DNA}^* / \pi \propto \eta^{3/2}$. Obviously, the conformational free energy of DNA biofilm is proportional to 3/2 power of the packing density of DNA chains, which is consistent with the results from Utz–Begley’s model [16].

2.2. Mechanical Energy

According to the linear elastic theory, the mechanical energy of non-biolyers can be written as [11]:

$$U_{bend} = \frac{1}{2} \int_0^l \int_0^b \left[\int_{-h/2}^{h_s-h/2} \sigma_s \epsilon dy + \int_{h_s-h/2}^{h/2-h_2} \sigma_1 \epsilon dy + \int_{h/2-h_2}^{h/2} \sigma_2 \epsilon dy \right] dx dz \tag{15}$$

where σ_s and σ_i ($i=1,2$) are the normal stresses in the Si- or SiN_x-, Ti- or Cr- and Au-layers, respectively.

The stress-strain relations for the non-biolyers are given as:

$$\sigma_s = E_s \epsilon, \quad \sigma_i = E_i \epsilon \tag{16}$$

Substituting Equations (11) and (16) into (15), the mechanical energy of non-biolyers are obtained as:

$$U_{bend} = \frac{lb}{48\rho^2} \left\{ E_s \left[(h + 2\epsilon_0\rho)^3 - (h - 2h_s + 2\epsilon_0\rho)^3 \right] + E_2 \left[(h - 2\epsilon_0\rho)^3 - (h - 2h_2 - 2\epsilon_0\rho)^3 \right] + E_1 \left[(h - 2h_s + 2\epsilon_0\rho)^3 - (2h_2 + 2\epsilon_0\rho - h)^3 \right] \right\} \tag{17}$$

Substituting Equations (14) and (17) into (1) yields the total free energy of microcantilever-based DNA sensors $\Pi = \Pi(\rho, \epsilon_0)$. The curvature radius ρ and the normal strain ϵ_0 could be obtained by the principle of minimum energy. In the sense of small curvature, the tip deflection w is predicted by [15]:

$$w = l^2 / (2\rho) \tag{18}$$

There are some differences between the present four-layered beam model and Utz–Begley’s [16] or Hagan’s [10] two-layered model. First, since the thicknesses of coating thin layers (e.g., the Au- and

Ti-layer) are smaller than that of substrate layer, the dedication of coating thin layers to the mechanical energy of microcantilever-based DNA sensors was neglected in Utz–Begley’s or Hagan’s model. However, the accuracy of an optical detection system has reached 0.1 nm [7]. Hence, it is necessary to set up the four-layered model for the more accurate prediction of deflections. Second, the conformational free energy of DNA biofilm is given with an improved scaling theory of thermal blobs considering the curvature effect of a soft substrate.

3. Results and Discussion

3.1. Effect of Curvature

The present model can be used to reveal the influence of the curvature effect of the substrate on the shape properties of DNA biofilm. From Equations (7) and (13), we define a dimensionless thickness ratio of DNA biofilm as:

$$\gamma = \frac{h_{\text{DNA}}}{h_{\text{DNA}}^*} = \frac{[1 + \epsilon_0 + 1 / (2\alpha)]^{\frac{v-1}{2v}}}{1 + \frac{1-v}{2v} \frac{\beta}{\alpha} [1 + \epsilon_0 + 1 / (2\alpha)]^{-\frac{v+1}{2v}}} \tag{19}$$

where $\alpha = \rho / h$, $\beta = h_{\text{DNA}}^* / h$. In the case of special conditions, Equation (19) could be further approximated as:

$$\gamma = \begin{cases} 1, & \epsilon_0 \approx 0, \beta / \alpha \ll 1 \text{ (Case 1)} \\ 1 - \frac{1-v}{2v} \frac{\beta}{\alpha}, & \epsilon_0 \approx 0, \beta / \alpha \gg 1 \text{ (Case 2)} \end{cases} \tag{20}$$

Figure 2. Thickness ratio of DNA biofilm $\gamma (= h_{\text{DNA}} / h_{\text{DNA}}^*)$ as a function of $\alpha (= \rho / h)$ under different nucleotide numbers.

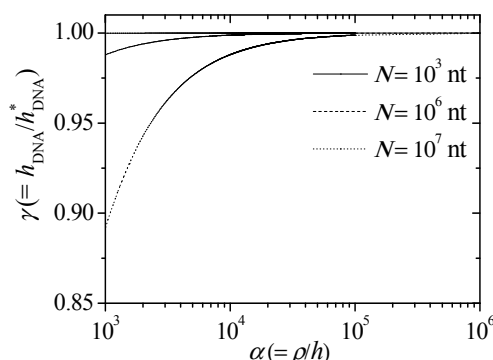


Figure 2 shows the thickness ratio of DNA biofilm γ as a function of α under different nucleotide numbers calculated from Equation (19) ($h_s = 1 \mu\text{m}$, $h_1 = 3 \text{ nm}$, $h_2 = 20 \text{ nm}$, $a = 0.22 \text{ nm}$, $v = 0.6$ [16], $\eta = 0.1 \text{ chain/nm}^2$, $\chi = 0$, $\epsilon_0 = 10^{-6}$). For short chain systems, such as in Case 1 ($N < 10^3 \text{ nt}$), the biofilm thickness almost does not change, that is to say, the curvature effect is small. For long chain systems in Case 2 ($N > 10^3 \text{ nt}$), the biofilm thickness almost retains no change for the substrate with a large curvature radius ($\rho/h > 10^5$), whereas it changes prominently for the substrate with a small curvature

radius ($\rho/h < 10^5$). This reason is that, for long chain systems with a small curvature radius of the substrate, DNA chains will occupy more space to decrease the biofilm thickness remarkably, in order to gain the global minimum of the free energy for the whole film-substrate system. In a word, the curvature effect seems weak in microcantilever-based DNA sensors, whereas it will become stronger in other substrate systems, such as nanocantilevers, membranes or gold nanoparticles. Due to a large application of microcantilever-based DNA sensors, next, we will investigate the effect of the chain length, the packing density of ssDNA and the thickness and elastic modulus of the substrate on the nanomechanical deflection of a microcantilever with short DNA chains.

3.2. Effect of Chain Length and Packing Density of ssDNA

The parameters are taken as $l = 200 \mu\text{m}$, $b = 20 \mu\text{m}$, $h_s = 0.5 \mu\text{m}$, $h_1 = 5 \text{ nm}$, $h_2 = 25 \text{ nm}$, $E_s = 180 \text{ GPa}$ [6], $E_1 = 140 \text{ GPa}$, $E_2 = 75 \text{ GPa}$ [26], $\chi = 0$, $k_B = 1.38 \times 10^{-23} \text{ J/K}$, $T = 298 \text{ K}$. Figure 3 shows the microcantilever deflection as a function of nucleotide number from the present model (*i.e.*, Equation (18)), Utz–Begley’s model [16], Hagan’s model [10] and Wu’s experimental data [6]. However, it should be mentioned that the DNA packing density was not measured in the experiments of Wu *et al.* [6]. In the preexisting literature, the packing density ranges either from 0.15 to 0.2 chain/nm² [10], or as high as 0.4 chain/nm² [8] or from 0.6 to 0.9 chain/nm² [27]. In Figure 3a, the packing density 0.4 chain/nm² is taken. The deflections predicted by Utz–Begley’s model are calculated based on their related work (see Equation (12) in [17]): $w = 3(1 - \mu_s)l^2\Delta\sigma / (E_s h_s^2)$, where $\Delta\sigma$ is the surface stress induced by molecular adsorption and $\mu_s (= 0.25)$ is the Poisson’s ratio of substrate layer.

Figure 3. Deflection of a microcantilever-based DNA sensor w as a function of nucleotide number N : (a) comparison of deflections predicted by different models; (b) comparison of deflections predicted by present model under different packing densities with Wu’s experimental data [6].

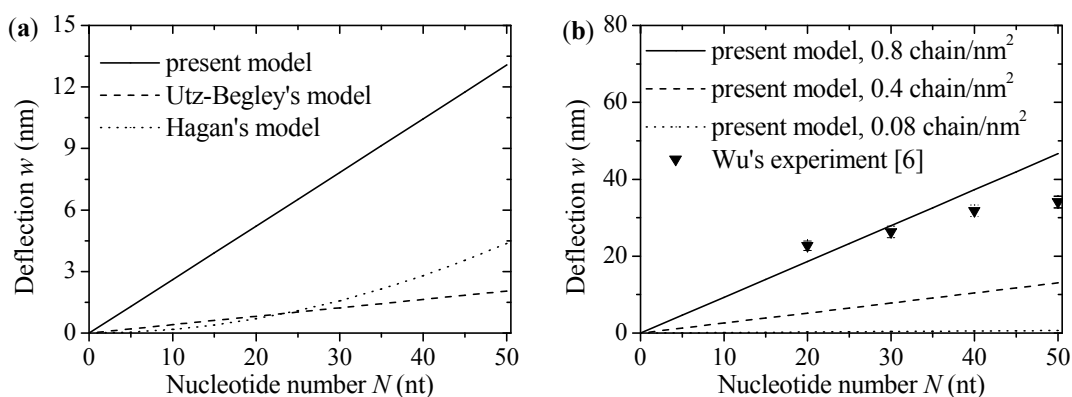


Figure 3a shows that the deflection increases with the enhancement of nucleotide number. The reason is that the contribution of the conformational free energy of DNA biofilm to the total free energy of the cantilever enhances with the increase of the nucleotide number, which makes the deflection increase. Figure 3b shows the comparison between deflection predictions by the present model under given packing densities of 0.08–0.8 chain/nm² and Wu’s experimental data (see the Figure 2a insert in [6]). Obviously, our model shows a lower error only at a packing density of 0.8 chain/nm². Note

that the conformational free energy is only one source of surface stress; the extension of the present work involving several other contributions (such as electrostatic forces, hydration forces or dispersion interactions) should be done in the near future and may offer better theoretical predictions.

Note that our model predicts almost an order of magnitude higher deflection (*i.e.*, about 10 nm difference) than the other two models. In fact, Utz–Begley’s model was developed specifically to separate the energies of the film from the continuum mechanical treatment of the substrate in order to allow correct treatment of multi-layered systems, membranes and other geometries. This assumption will possibly make their predictions invalid in the case of nanostructure system with large curvature. In addition, their model only involves the vertical forces applied along DNA chains and ignored the interaction between neighboring DNA molecules. However, Shi *et al.* [31] found that, in the case of macromolecules adsorption (including ssDNA adsorption), the normal stiffness is usually very small; the interaction between the neighboring macromolecules dominates the overall bending stiffness. Hence, following Hagan’s approach [10], we discuss the conformational free energy of DNA film on the deformed configuration obtained by the principle of minimum energy. The advantage of the principle of minimum energy is obvious, because it is not necessary to distinguish between the directions of surface stress induced by DNA adsorptions. Meanwhile, different from the viewpoint of Hagan *et al.* [10], we discussed adsorption-induced deflections by considering the thermal blob theory. Thus, these differences in modeling approaches result in a bigger deflection predicted by our model. Note that an optical beam deflection technique employed in the sensor has an accuracy of 0.1 nm [7]. In addition, the studies of noise signals have shown that the variations of controlled temperature and ion concentration in aqueous solutions could only produce deflections of 2–5 nm [6,28]. Therefore, the effect of conformational entropy on deflections could not be neglected.

Figure 4. Deflection of a microcantilever-based DNA sensor w as a function of packing density η ($N = 30$ nt, $\chi = 0$).

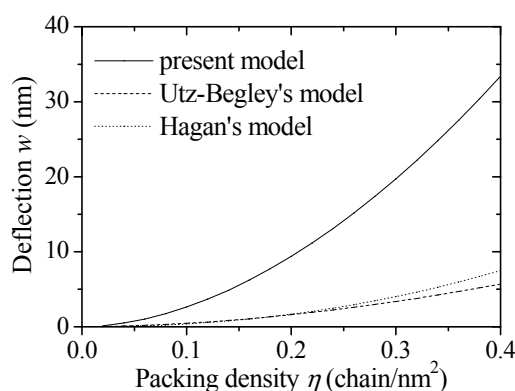


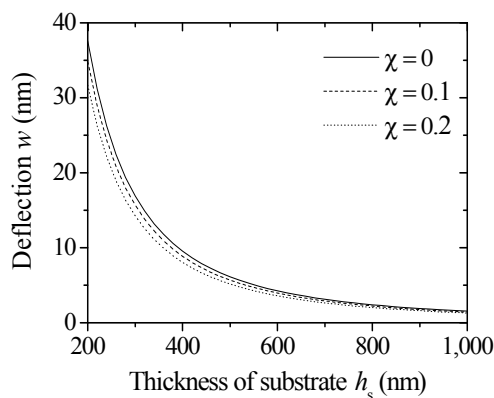
Figure 4 shows the effect of the packing density of DNA chains on microcantilever deflections predicted by the present model, Utz–Begley’s model [16] and Hagan’s model [10]. The parameters are taken as $l = 300 \mu\text{m}$, $b = 40 \mu\text{m}$, $h_s = 0.5 \mu\text{m}$, $h_1 = 5 \text{ nm}$, $h_2 = 25 \text{ nm}$, $E_s = 85 \text{ GPa}$, $E_1 = 140 \text{ GPa}$, $E_2 = 73 \text{ GPa}$ [29,30]. The deflection grows with the increase of packing density. As the packing density increases, the contribution of conformational free energy enhances with the incremental thickness of DNA biofilm; this causes the deflection to increase. In Utz–Begley’s model and Hagan’s

model, the effect of packing density on deflection seems small, while the deflection predicted by the present model follows an exponential relation with packing density. Unfortunately, we cannot compare these predictions with Stachowiak's experimental values [29], because immobilization deflections (a linear function of surface stress) were not recorded. It should be noted that surface stress increases monotonically with packing density (see the Figure 7b insert in [29]). This tendency found in the experiment is the same as our prediction in Figure 4.

3.3. Effect of Thickness and Elastic Modulus of Substrate

In order to improve the sensitivity and reliability of biosensors, an approach of changing the geometry profile or material of substrates has been developed. The effect of the thickness and elastic modulus of the substrate on deflections will be discussed. In the following numerical example, the parameters are taken as $l = 750 \mu\text{m}$, $b = 100 \mu\text{m}$, $h_s = 1 \mu\text{m}$, $h_1 = 3 \text{ nm}$, $h_2 = 20 \text{ nm}$, $E_s = 169 \text{ GPa}$ [8], $E_1 = 116 \text{ GPa}$, $E_2 = 78 \text{ GPa}$. Figure 5 shows the microcantilever deflection as a function of the thickness of the substrate under given Flory interaction parameters ($\eta = 0.08 \text{ chain/nm}^2$, $N = 30 \text{ nt}$). The deflection decreases remarkably with the increase of substrate thickness. With the increase of substrate thickness, the bending stiffness of non-bilayers also increases; this reduces the relative contribution of the conformational free energy of DNA biofilm to nanomechanical motion. Therefore, it is desirable to make the cantilever as thin as possible to improve the deflection signal. In addition, as the Flory interaction parameter decreases, the deflection increases. The reason is that, for low Flory interaction parameters, DNA chains in good solvents will take more extended conformations and move away from the cantilever surface. Note that the cantilever is a deformable structure, and the curvature allows each chain to occupy a larger lateral space as the distance from the surface increases. The systems with more extended conformations experience a larger driving force to deflect. Thus, the deflection becomes larger with the decrease of the Flory parameter.

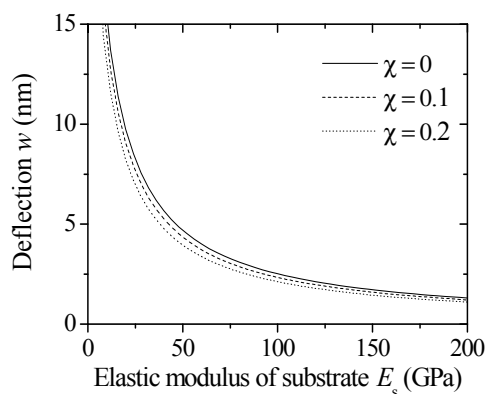
Figure 5. Deflection of a microcantilever-based DNA sensor w as a function of the thickness of substrate h_s under different Flory interaction parameters χ ($\eta = 0.08 \text{ chain/nm}^2$, $N = 30 \text{ nt}$).



In addition to the change of cantilever geometry, the material selection can also be used to improve the sensitivity of biosensors. The related parameters are the same as those in Figure 5. Figure 6 shows the microcantilever deflection as a function of the elastic modulus of the substrate under given Flory

interaction parameters ($\eta = 0.08$ chain/nm², $N = 30$ nt). The deflection decreases with the increase of the elastic modulus of the substrate due to high bending stiffness values. Therefore, in order to enhance the deflection signal, low elastic modulus materials (e.g., SU-8 polymer material [32], *i.e.*, a photopolymerizable epoxy-acrylate polymer) could be used as the substrate.

Figure 6. Deflection of a microcantilever-based DNA sensor w as a function of the elastic modulus of the substrate E_s under different Flory interaction parameters χ ($\eta = 0.08$ chain/nm², $N = 30$ nt).



4. Conclusions

A four-layered beam model for microcantilever deflections induced by conformational free energy is formulated by extending the scaling theory for ssDNA brushes and Zhang's two-variable method for laminated cantilever beams. The relationship among cantilever deflection, the characteristics of ssDNA molecules, the mechanical properties of deformable substrate, *etc.*, are established by the principle of minimum energy. Results show that the effect of conformational entropy on microcantilever deflections cannot be ignored, especially at the conditions of high packing density or long chain systems. In addition, in order to improve the sensitivity of biosensors, it should be as small as possible to reduce the substrate stiffness. A comparison of different models shows that the deflections by the proposed analytical model appear quantitatively closer to the related experimental values. It should be noted that the conformational entropy is only one of several factors; several important issues remain unsettled. For example, highly-charged DNA molecules can directly repel each other via electrostatic or hydration forces in other circumstances. The situation in ssDNA systems will be more complicated than in dsDNA systems [2,33–36]. Therefore, it is necessary to investigate the influence of other interactions on deflections or to develop other models for ssDNA in the future.

Acknowledgments

The research was supported by the Natural Science Foundation of China (No. 10872121 and No. 11272193), the Shanghai Leading Academic Discipline Project (No. S30106) and the Scientific Research Foundation of Changzhou University (No. ZMF14020058).

Author Contributions

Zou-Qing Tan and Neng-Hui Zhang conceived of the elaboration of the paper through all of the stages. Both authors cooperated in the analysis and interpretation of the data and the writing and revision of the paper. Both authors have read and approved the final manuscript.

Conflicts of Interest

The authors declare no conflict of interest.

References

1. Huber, F.; Lang, H.P.; Backmann, N.; Rimoldi, D.; Gerber, C. Direct detection of a BRAF mutation in total RNA from melanoma cells using cantilever arrays. *Nat. Nanotechnol.* **2013**, *8*, 125–129.
2. Zhang, N.H.; Tan, Z.Q.; Li, J.J.; Meng, W.L.; Xu, L.W. Interactions of single-stranded DNA on microcantilevers. *Curr. Opin. Colloid Interface Sci.* **2011**, *16*, 592–596.
3. Arlett, J.L.; Myers, E.B.; Roukes, M.L. Comparative advantages of mechanical biosensors. *Nat. Nanotechnol.* **2011**, *6*, 203–215.
4. Fritz, J.; Baller, M.K.; Lang, H.P.; Rothuizen, H.; Vettiger, P.; Meyer, E.; Guntherodt, H.J.; Gerber, C.; Gimzewski, J.K. Translating biomolecular recognition into nanomechanics. *Science* **2000**, *288*, 316–318.
5. Braun, T.; Ghatkesar, M.K.; Backmann, N.; Grange, W.; Boulanger, P.; Letellier, L.; Lang, H.P.; Bietsch, A.; Gerber, C.; Hegner, M. Quantitative time-resolved measurement of membrane protein-ligand interactions using microcantilever array sensors. *Nat. Nanotechnol.* **2009**, *4*, 179–185.
6. Wu, G.H.; Ji, H.F.; Hansen, K.; Thundat, T.; Datar, R.; Cote, R.; Hagan, M.F.; Chakraborty, A.K.; Majumdar, A. Origin of nanomechanical cantilever motion generated from biomolecular interactions. *Proc. Natl. Acad. Sci. USA.* **2001**, *98*, 1560–1564.
7. McKendry, R.; Zhang, J.Y.; Arntz, Y.; Strunz, T.; Hegner, M.; Lang, H.P.; Baller, M.K.; Certa, U.; Meyer, E.; Guntherodt, H.J.; Gerber, C. Multiple label-free biodetection and quantitative DNA-binding assays on a nanomechanical cantilever array. *Proc. Natl. Acad. Sci. USA.* **2002**, *99*, 9783–9788.
8. Mertens, J.; Rogero, C.; Calleja, M.; Ramos, D.; Martin-Gago, J.A.; Briones, C.; Tamayo, J. Label-free detection of DNA hybridization based on hydration-induced tension in nucleic acid films. *Nat. Nanotechnol.* **2008**, *3*, 301–307.
9. Sushko, M.L.; Harding, J.H.; Shluger, A.L.; McKendry, R.A.; Watari, M. Physics of nanomechanical biosensing on cantilever arrays. *Adv. Mater.* **2008**, *20*, 3848–3853.
10. Hagan, M.F.; Majumdar, A.; Chakraborty, A.K. Nanomechanical forces generated by surface grafted DNA. *J. Phys. Chem. B* **2002**, *106*, 10163–10173.
11. Zhang, N.H.; Shan, J.Y. An energy model for nanomechanical deflection of cantilever-DNA chip. *J. Mech. Phys. Solids* **2008**, *56*, 2328–2337.

12. Liu, F.; Zhang, Y.; Ou-Yang, Z.C. Flexoelectric origin of nanomechanic deflection in DNA-microcantilever system. *Biosens. Bioelectron.* **2003**, *18*, 655–660.
13. Begley, M.R.; Utz, M.; Komaragiri, U. Chemo-mechanical interactions between adsorbed molecules and thin elastic films. *J. Mech. Phys. Solids* **2005**, *53*, 2119–2140.
14. Sushko, M.L. Nanomechanics of organic/inorganic interfaces: A theoretical insight. *Faraday Discuss.* **2009**, *143*, 63–80.
15. Zhang, N.H.; Shan, J.Y.; Xing, J.J. Piezoelectric properties of single-strand DNA molecular brush bilayers. *Acta Mech. Solida Sin.* **2007**, *20*, 206–210.
16. Utz, M.; Begley, M.R. Scaling theory of adsorption-induced stresses in polymer brushes grafted onto compliant structures. *J. Mech. Phys. Solids* **2008**, *56*, 801–814.
17. Begley, M.R.; Utz, M. Multiscale modeling of adsorbed molecules on freestanding microfabricated structures. *J. Appl. Mech.* **2008**, *75*, doi:10.1115/1.2793130.
18. Hariharan, R.; Biver, C.; Mays, J.; Russel, W.B. Ionic strength and curvature effects in flat and highly curved polyelectrolyte brushes. *Macromolecules* **1998**, *31*, 7506–7513.
19. Rubinstein, M.; Colby, R.H. *Polymer Physics*; Oxford University Press: Oxford, UK, 2003.
20. Zhang, N.H.; Xing, J.J. An alternative model for elastic bending deformation of multilayered beams. *J. Appl. Phys.* **2006**, *100*, doi:10.1063/1.2372578.
21. Zhang, N.H. Thermoelastic stresses in multilayered beams. *Thin Solid Films* **2007**, *515*, 8402–8406.
22. Zhang, N.H.; Chen, J.Z. An alternative two-variable model for bending problems of multilayered beams. *J. Appl. Mech.* **2008**, *75*, doi:10.1115/1.2912994.
23. Zhang, N.H.; Chen, J.Z. Elastic bending analysis of bilayered beams by an alternative two-variable method. *Eur. J. Mech. A* **2009**, *28*, 284–288.
24. Zhang, N.H.; Chen, J.Z. An alternative model for elastic thermal stresses in two materials joined by a graded layer. *Compos. Part B.* **2010**, *41*, 375–379.
25. Zhang, N.H.; Meng, W.L.; Aifantis, E.C. Elastic bending analysis of bilayered beams containing a gradient layer by an alternative two-variable method. *Compos. Struct.* **2011**, *93*, 3130–3139.
26. Herrera-May, A.L.; Aguilera-Cortes, L.A.; Plascencia-Mora, H.; Rodriguez-Morales, A.L.; Lu, J. Analytical modeling for the bending resonant frequency of multilayered microresonators with variable cross-section. *Sensors* **2011**, *11*, 8203–8226.
27. Steel, A.B.; Levicky, R.L.; Herne, T.M.; Tarlov, M.J. Immobilization of nucleic acids at solid surfaces: Effect of oligonucleotide length on layer assembly. *Biophys. J.* **2000**, *79*, 975–981.
28. Alvarez, M.; Carrascosa, L.G.; Moreno, M.; Calle, A.; Zaballos, A.; Lechuga, L.M.; Martinez, A.C.; Tamayo, J. Nanomechanics of the formation of DNA self-assembled monolayers and hybridization on microcantilevers. *Langmuir* **2004**, *20*, 9663–9668.
29. Stachowiak, J.C.; Yue, M.; Castelino, K.; Chakraborty, A.; Majumdar, A. Chemomechanics of surface stresses induced by DNA hybridization. *Langmuir* **2006**, *22*, 263–268.
30. Yue, M.; Lin, H.; Dedrick, D.E.; Satyanarayana, S.; Majumdar, A.; Bedekar, A.S.; Jenkins, J.W.; Sundaram, S. A 2-D microcantilever array for multiplexed biomolecular analysis. *J. Microelectromech. Syst.* **2004**, *13*, 290–299.
31. Shi, M.X.; Liu, B.; Zhang, Z.Q.; Zhang, Y.W.; Gao, H.J. Direct influence of residual stress on the bending stiffness of cantilever beams. *Proc. R. Soc. A* **2012**, *468*, 2595–2613.

32. Calleja, M.; Tamayo, J.; Nordstrom, M.; Boisen, A. Low-noise polymeric nanomechanical biosensors. *Appl. Phys. Lett.* **2006**, *88*, doi:10.1063/1.2187437.
33. Zhang, N.H.; Meng, W.L.; Tan, Z.Q. A multi-scale model for the analysis of the inhomogeneity of elastic properties of DNA biofilm on microcantilevers. *Biomaterials* **2013**, *34*, 1833–1842.
34. Zhang, N.H.; Chen, J.Z.; Li, J.J.; Tan, Z.Q. Mechanical properties of DNA biofilms adsorbed on microcantilevers in label-free biodetections. *Biomaterials* **2010**, *31*, 6659–6666.
35. Tang, H.S.; Meng, W.L.; Zhang, N.H. Mechanical properties of double-stranded DNA biofilm with Gaussian distribution. *Acta Mech. Sin.* **2014**, *30*, 15–19.
36. Meng, W.L.; Tan, Z.Q.; Tang, H.S.; Zhang, N.H. Elastic properties of single-stranded DNA biofilm with strong interactions. In Proceedings of Sixth International Conference on Nonlinear Mechanics (ICNM-6), Shanghai, China, 12–15 August 2013; Zhou, Z.W., Ed.; DES Tech Publications: Lancaster, PA, USA, 2013; pp. 154–157.

© 2014 by the authors; licensee MDPI, Basel, Switzerland. This article is an open access article distributed under the terms and conditions of the Creative Commons Attribution license (<http://creativecommons.org/licenses/by/3.0/>).